Inter*net* Electronic Journal*

Nanociencia et Moletrónica

Diciembre 2006, Vol. 4, N°3, pp. 729-742

All-optical switching and slow light in photonic crystals

A. Miroshnichenko[1], S. Mingaleev[2,3], K. Busch[2], and Y. Kivshar[1]

[1]Nonlinear Physics Centre, Research School of Physical Sciences and Engineering,
Australian National University, Canberra ACT 0200, Australia and
[2]Institut for Theoretische Festkörperphysik, Universitaet Karlsruhe, Germany
[3]Bogolyubov Institute for Theoretical Physics of the National Academy of Sciences of Ukraine,
03143 Kiev, Ukraine

recibido: 29 Octubre 2006 revisado: 30 Octubre 2006 publicado: 15 de Noviembre de 2006

Citation of the article:
A. Miroshnichenko, S. Mingaleev, K. Busch, and Y. Kivshar, All-optical switching and slow light in photonic crystals, Internet Electrón. J. Nanocs. Moletrón. 2006, Vol. 4, N° 3., pp 729-742

All-optical switching and slow light in photonic crystals

A. Miroshnichenko[1], S. Mingaleev[2,3], K. Busch[2], and Y. Kivshar[1]

[1]Nonlinear Physics Centre, Research School of Physical Sciences and Engineering,
Australian National University, Canberra ACT 0200, Australia and
[2]Institut for Theoretische Festkörperphysik, Universitaet Karlsruhe, Germany
[3]Bogolyubov Institute for Theoretical Physics of the National Academy of Sciences of Ukraine,
03143 Kiev, Ukraine

recibido: 29 Octubre 2006 revisado: 30 Octubre 2006 publicado: 15 de Noviembre de 2006

Internet Electron. J. Nanoc. Moletrón. 2006, Vol. 4, No.3, pags. 729-742

Abstract

We analyze resonant transmission in photonic-crystal waveguides coupled to nonlinear resonators. We reveal that the discrete nature of the photonic-crystal structures allows for a novel, geometry-mediated enhancement of nonlinear effects, based on the high-Q side-coupled nonlinear resonators, which can be useful for a design of all-optical slow-light photonic devices.

I. INTRODUCTION

Future integrated photonic circuits for ultrafast all-optical signal processing would require different types of nonlinear functional elements such as light switchers, memory, and logic devices. Therefore, both novel physics and novel designs of such all-optical devices have attracted a significant research in photonics during last two decades, and most of these studies utilize the concepts of optical switching and bistability [1].

One of the simplest bistable optical devices which can find applications in integrated photonic circuits [2] is a two-port device which is connected to other parts of a circuit by one input and one output waveguides. Due to a periodic modulation of the refractive index, such structures may possess complete *photonic band gaps*, i.e. the regions of optical frequencies where PhCs act as ideal optical insulators. In this work, we study photonic-crystal waveguides side-coupled to Kerr nonlinear resonators [3]-[10] (see Fig. 1) which may serve as the basic elements of an active photonic-crystal circuitry. We obtain explicit analytical expressions for the bistability thresholds and transmission coefficients related to the light switching in such structures. We develop an improved semi-analytical approach based on the effective discrete equations derived in the framework of a consistent Green's function formalism [11]–[14]. This novel approach allows us to describe adequately light transmission in the waveguide-resonator structures near the band edges.

In addition. we show how to employ geometry-driven enhancement of nonlinearity [15]–[17] and, simultaneously, a substantial reduction of the bistability threshold [18]. The possibility of such enhancement is a direct consequence of the discreteness of the waveguides. We demonstrate how the engineering of the geometry of photonic-crystal becomes extremely useful for developing of novel concepts of all-optical switching in the slow-light regime of the photonic-crystal waveguides.

The paper is organized as follows. In Sec. II.A we derive a system of the effective discrete nonlinear equations [13, 14] and utilize the recently developed approach for its analysis [15, 16]. Specifically, in Sec. II.B we study the intersite waveguide-resonator geometry, schematically depicted in Fig. 1. In Sec. III, we illustrate our main findings by several examples of the specific optical devices based on a two-dimensional photonic crystal created by a square lattice of Si rods. Finally, in Sec. IV we summarizes our results.

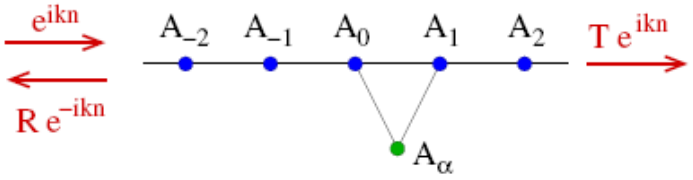

FIG. 1: Schematic of a straight waveguide in a photonic crystal side-coupled to a nonlinear optical resonator. Solid lines show the major interactions.

II. WAVEGUIDE-RESONATOR STRUCTURE

We study the transmission properties of the photonic-crystal waveguide with a side-coupled nonlinear resonator. It was shown that such a structure may demonstrate the resonant reflection [5, 6] or the Fano resonance [19] with a large Q factor. Based of the analytical results [15, 18], we find below that for the coupled-resonator-optical-waveguide (CROW) geometry it is possible to achieve extremely large values of the Q factor that leads to the low bistability threshold in the nonlinear regime.

A. Discrete Equations

First, we derive an appropriate set of discrete equations, and show that they can be applied to a variety of the photonic-crystal devices. We start from the wave equation in the frequency domain for the electric field

$$\left[\vec{\nabla}\times\vec{\nabla}\times-\left(\frac{\omega}{c}\right)^2\hat{\varepsilon}(\vec{r})\right]\vec{E}(\vec{r})=0\,, \tag{1}$$

where the dielectric function $\hat{\varepsilon}(\vec{r})=\hat{\varepsilon}_{\rm pc}(\vec{r})+\delta\hat{\varepsilon}(\vec{r})$ consists of the dielectric function $\hat{\varepsilon}_{\rm pc}(\vec{r})$ of a perfectly periodic structure and a perturbation $\delta\hat{\varepsilon}(\vec{r})$ that describes the embedded cavities. It is convenient to introduce the tensorial Green function of the perfectly periodic photonic crystal,

$$\left[\vec{\nabla}\times\vec{\nabla}\times-\left(\frac{\omega}{c}\right)^2\hat{\varepsilon}_{\rm pc}(\vec{r})\right]\hat{G}(\vec{r},\vec{r}\,'|\omega)=\hat{I}\delta(\vec{r}-\vec{r}\,') \tag{2}$$

and to rewrite Eq. (1) in the integral form,

$$\vec{E}(\vec{r})=\left(\frac{\omega}{c}\right)^2\int\vec{r}\,'\,\hat{G}(\vec{r},\vec{r}\,'|\omega)\,\delta\hat{\varepsilon}(\vec{r}\,')\,\vec{E}(\vec{r}\,')\,, \tag{3}$$

where we assume that the frequency ω lies inside a complete photonic bandgap so that the electric field vanishes everywhere except for areas inside and in the vicinity of cavities. We enumerate the cavities by an integer index n and introduce dimensionless functions $\theta_n(\vec{r})$ which describe the shape of the n-th cavity. As a result, $\delta\hat{\varepsilon}(\vec{r})$ may be represented as

$$\delta\hat{\varepsilon}(\vec{r}) = \sum_n \left[\delta\hat{\varepsilon}_n + \chi_n^{(3)}|\vec{E}(\vec{r})|^2\right] \theta_n(\vec{r} - \vec{R}_n) \,, \tag{4}$$

where $\vec{R}_n$, $\delta\hat{\varepsilon}_n$, and $\chi_n^{(3)}$ are, respectively, position, (linear) dielectric function, and nonlinear third-order susceptibility of the n-th cavity.

We describe the electric field of the n-th cavity mode via a dimensionless field profile $\vec{\mathcal{E}}_n(\vec{r})$ and a complex amplitude A_n. Taking into account that *inside* the cavities the electric field of the system is a superposition

$$\vec{E}(\vec{r}) \simeq \sum_n A_n \, \vec{\mathcal{E}}_n(\vec{r} - \vec{R}_n) \,, \tag{5}$$

Eq. (3) can be rewritten as a set of discrete nonlinear equations

$$D_n(\omega)A_n = \sum_{m\neq n} V_{n,m}(\omega)A_m + \kappa_n(\omega)\chi_n^{(3)}|A_n|^2 A_n, \tag{6}$$

where $D_n(\omega) = 1 - V_{n,n}(\omega)$ is the dimensionless frequency detuning from the resonance frequency, ω_n, of the n-th cavity. Furthermore,

$$\begin{aligned} V_{n,m}(\omega) \;=\; & \frac{\delta\varepsilon_m}{W_n}\left(\frac{\omega}{c}\right)^2 \int d\vec{r} \int d\vec{r}' \; \vec{\mathcal{E}}_n^*(\vec{r})\hat{\varepsilon}_n(\vec{r}) \\ & \times \; \theta_m(\vec{r}')\hat{G}(\vec{r} + \vec{R}_n - \vec{R}_m, \vec{r}'|\omega) \, \vec{\mathcal{E}}_m(\vec{r}') \,, \end{aligned} \tag{7}$$

is the dimensionless linear coupling between the n-th and the m-th cavity. Similarly,

$$\begin{aligned} \kappa_n(\omega) \;=\; & \frac{1}{W_n}\left(\frac{\omega}{c}\right)^2 \int d\vec{r} \int d\vec{r}' \; \vec{\mathcal{E}}_n^*(\vec{r})\hat{\varepsilon}_n(\vec{r}) \\ & \times \; \theta_n(\vec{r}')\hat{G}(\vec{r}, \vec{r}'|\omega) \, |\vec{\mathcal{E}}_n(\vec{r}')|^2 \vec{\mathcal{E}}_n(\vec{r}') \,, \end{aligned} \tag{8}$$

is the dimensionless and scale-invariant *nonlinear feedback parameter* which should be compared with the analogous parameter, introduced in the conventional coupled-mode theory analysis [5, 7]. Finally, W_n is defined as

$$W_n = \int_{\text{allspace}} d\vec{r} \, \varepsilon_a(\vec{r})|\vec{\mathcal{E}}_n(\vec{r})|^2 \,. \tag{9}$$

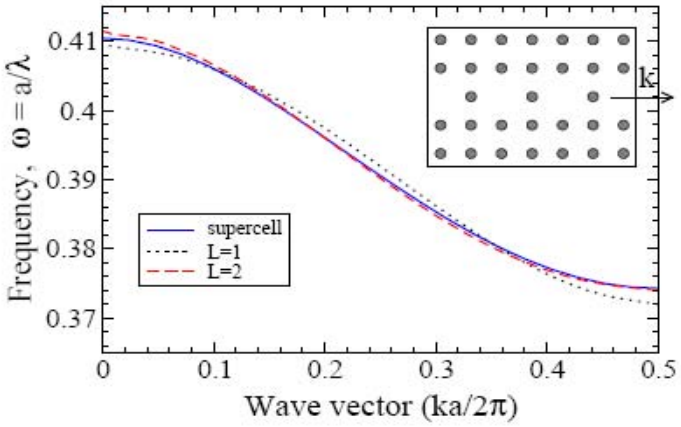

FIG. 2: CROW waveguide dispersion.

We remark that in deriving Eqs. (6) we have neglected higher-order couplings proportional to the integrals of $\vec{\mathcal{E}}_n^*(\vec{r})\vec{\mathcal{E}}_m(\vec{r}+\vec{R}_n-\vec{R}_m)$ with $n \neq m$ but take into account the coupling coefficients which involve integrals of $\hat{G}(\vec{r}+\vec{R}_n-\vec{R}_m,\vec{r}'|\omega)$ with $n \neq m$.

Here, we apply Eqs. (6)–(8) to study the more complicated case of the nonlinear coupled waveguide-resonator systems. The set of Eqs. (6) may be separated in this case according to

$$\begin{aligned} D_{\rm w}(\omega)A_n &= \sum_{j=1}^{L} V_{jw}(\omega)(A_{n+j}+A_{n-j}) + V_{n,\alpha}(\omega)A_\alpha \,, \\ D_\alpha(\omega)A_\alpha &= \sum_j V_{\alpha,j}(\omega)A_j + \kappa_\alpha(\omega)\chi_\alpha^{(3)}|A_\alpha|^2 A_\alpha \,, \end{aligned} \tag{10}$$

where we assume that all cavities of the photonic-crystal waveguide are identical and linear, so that we can denote $D_{\rm w}(\omega) \equiv D_n(\omega)$ and $V_{jw}(\omega) \equiv V_{n,n\pm j}(\omega)$ for any n inside the waveguide. Furthermore, the index α defines the parameters of the side-coupled nonlinear resonator. The dispersion of the waveguide is shown on Fig.2.

To study the transmission property we impose the scattering boundary condition for the first equation in Eq. (10)

$$A_n = I_{\rm in}^{1/2} \begin{cases} t(\omega)\, e^{ik(\omega)sn} & n \gg 1 \,, \\ e^{ik(\omega)sn} + r(\omega)\, e^{-ik(\omega)sn} & n \ll -1 \,, \end{cases} \tag{11}$$

where s is the distance between the nearest waveguide cavities and $I_{\rm in}$ is the intensity of the incoming light.

B. Inter-site resonator

We consider the situation where the α-resonator is placed *symmetrically* between two cavities of the waveguide and, therefore, couples equally to both of them [see Fig. 1]. Assuming that in this case the nonvanishing coupling coefficients in Eq. (10) are $V_{1w}(\omega)$, $V_{\alpha,1}(\omega) \equiv V_{\alpha,0}(\omega)$, and $V_{1,\alpha}(\omega) \equiv V_{0,\alpha}(\omega)$, we seek solutions to the first equation of the system (10) that are of the form of Eq. (11). We look for the transmission and reflection coefficients in the following form [18]

$$T = \frac{[\sigma(\omega) - \mathcal{J}_\alpha]^2}{[\sigma(\omega) - \mathcal{J}_\alpha]^2 + 1} , \quad R = \frac{1}{[\sigma(\omega) - \mathcal{J}_\alpha]^2 + 1} . \tag{12}$$

It is easy to see that $T + R = 1$ for any $\sigma(\omega)$. Here, $\mathcal{J}_\alpha$ is a new dimensionless parameter which is proportional to the intensity of the resonator's localized mode

$$\mathcal{J}_\alpha = \frac{12\pi Q\,\kappa}{W_\alpha^2}\chi_\alpha^{(3)}|A_\alpha|^2 . \tag{13}$$

We find the generalized intensity-dependent frequency detuning in following form

$$\sigma(\omega) + \mathcal{J}_\alpha = i - i\left(e^{ik(\omega)s} - 1\right)\frac{V_{1w}(\omega)}{V_{0,\alpha}(\omega)}\frac{I_{in}^{1/2}}{A_\alpha} . \tag{14}$$

The corresponding amplitudes are

$$\begin{aligned} A_0 &= I_{in}^{1/2} - \frac{1}{[1 - e^{-ik(\omega)s}]}\frac{V_{0,\alpha}(\omega)}{V_{1w}(\omega)}A_\alpha , \\ A_1 &= e^{ik(\omega)s}I_{in}^{1/2} - \frac{1}{[1 - e^{-ik(\omega)s}]}\frac{V_{0,\alpha}(\omega)}{V_{1w}(\omega)}A_\alpha . \end{aligned} \tag{15}$$

Despite the complex form of Eq. (14), we would like to emphasize that the detuning $\sigma(\omega)$ determined by Eq. (14) is a *real-valued* function.

In the case of the linear α-resonator (i.e., for $\chi_\alpha^{(3)} \equiv 0$), we obtain

$$\sigma(\omega) = [1 + \mu(\omega)]\tan\left(\frac{k(\omega)s}{2}\right) , \tag{16}$$

where $\mu(\omega)$ is given by

$$\mu(\omega) = \frac{D_\alpha(\omega)V_{1w}(\omega)}{V_{0,\alpha}(\omega)V_{\alpha,0}(\omega)} . \tag{17}$$

For a high-quality α-resonator in the vicinity of the resonance frequency the corresponding quality factor can be approximated as

$$Q \approx \frac{V_{1w}\tan[k(\omega_{res})s/2]}{2\,\nu_\alpha\,V_{0,\alpha}V_{\alpha,0}} , \tag{18}$$

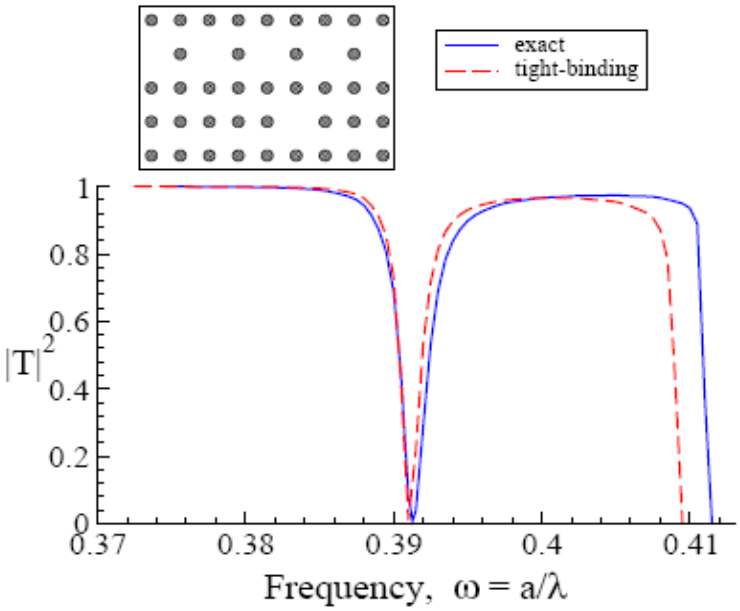

FIG. 3: Liner transmission through a photonic crystal waveguide created by removing every second rod in a row ($\vec{s} = 2\vec{a}_1$) side-coupled to an inter-site resonator created by removing a single rod. We compare exact numerical results (solid line) with the analytical results based on Eq. (16) (dashed line).

which is proportional to the factor $\tan[ks/2]$ which does not vanish and even diverges as $k(\omega_{\rm res})$ approaches the edge of the transmission band $k = \pm\pi/s$. At this band edge, $\sigma(\omega) \sim \tan(k(\omega)s/2) \to \infty$ and, therefore, light transmission is always perfect. This conclusion is supported by the exact numerical calculations presented in Fig. 3. At the other band edge, i.e., for $k(\omega) = 0$, transmission vanishes.

The light intensity at the α-resonator reaches its maximal value at the resonance frequency

$$|A_\alpha(\omega_{\rm res})|^2 \simeq 4\left(\frac{V_{1w}}{V_{0,\alpha}}\right)^2 \sin^2\left[\frac{k(\omega_{\rm res})s}{2}\right] \cdot I_{\rm in}$$
$$\simeq \left(4Q\nu_\alpha V_{\alpha,0}\cos\left[\frac{k(\omega_{\rm res})s}{2}\right]\right)^2 \cdot I_{\rm in} \qquad (19)$$

We note, that Eq. (19) does not vanish at the edge of the transmission band $k = \pm\pi/s$. Therefore, we can expect that for inter-site coupled structure nonlinear effects at the band edge $k = \pm\pi/s$ should be sufficiently strong to allow bistable transmission and switching. Therefore, this structure may be utilized for realizing efficient all-optical switching devices

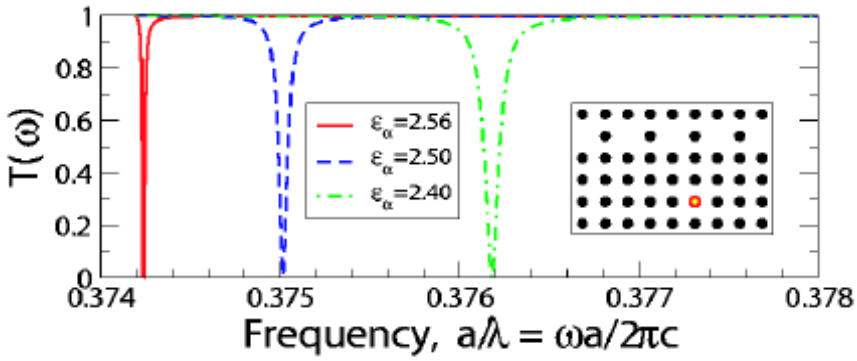

FIG. 4: (Color online) Linear transmission spectrum for a photonic crystal waveguide created by removing every second rod in a row ($\vec{s} = 2\vec{a}_1$) side-coupled to an inter-site polymer-rod resonator (marked by the open circle in the insets). The results for three different values of the resonator dielectric constant ε_α are shown.

based on *slow-light photonic crystal waveguides*.

III. SWITCHING AND BISTABILITY

We consider a two-dimensional photonic crystal created by a square lattice of dielectric rods in air. The rods are made from Si or $GaAs$ ($\varepsilon = 11.56$) and have radius $r = 0.18a$.

First, we consider a waveguide created by removing *every second rod* ($s = 2a$) in a straight line of rods coupled to a nonlinear resonator α created by replacing a single rod of the two-dimensional lattice with a highly-nonlinear polymer rod. The corresponding structure is schematically shown in the insets in Fig. 4. The resonant frequency of the polymer-rod resonator lies very close to the edge $k = \pm\pi/s$ of the waveguide passing band, and can be tuned by changing the linear dielectric constant ε_α of the rod.

In Fig. 4, we display the transmission spectra for inter-site positions of the side-coupled resonator for three different values of resonator dielectric constant ε_α.

The bistability may be realized for the inter-site position of the side-coupled resonator for which the transmission remains perfect at the band edge $k = \pm\pi/s$ and the quality factor Q increases as the resonant frequency approaches this band edge. In Fig. 5(b) (example A) we show that in this case bistable transmission indeed occurs for the frequency marked by a filled circle in Fig. 5(a). This corresponds to $T(\omega) = 80\%$.

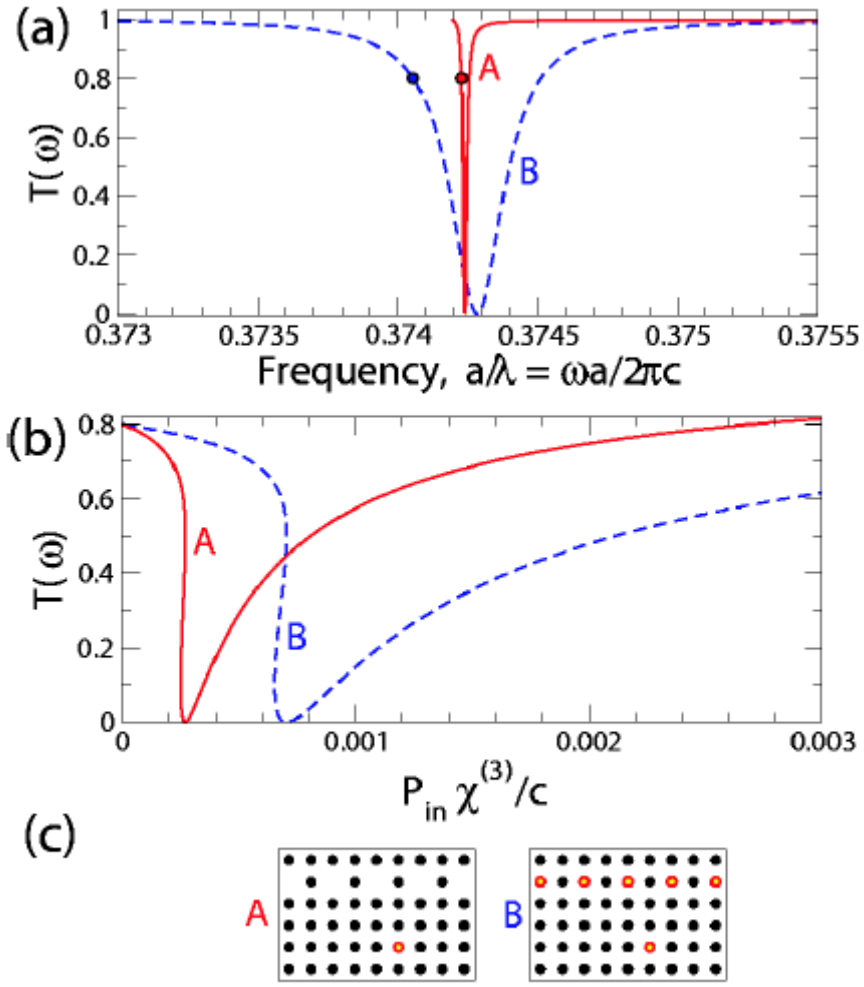

FIG. 5: (a) Linear transmission spectrum and (b) nonlinear bistable transmission for three different side-coupled waveguide-resonator photonic crystal structures whose topology is shown in (c). The rods consist of Si or GaAs (full black circles) or polymer (open red circles). Example A represents a close to optimal structure with *inter-site* location of the α-resonator whose resonance frequency lies close to the edge $k = \pm\pi/s$ of the passing band; example B represents a sub-optimal structure with an *inter-site* location of the α-resonator whose resonance frequency lies near the center of the passing band. Closed circles in (a) indicate frequencies with $T(\omega) = 80\%$ that are used for achieving high-contrast bistability in (b). Red circles in (c) indicate positions of the nonlinear polymer rods with $\varepsilon_\alpha = 2.56$.

We want to emphasize that the large value of the quality factor (18) for the inter-site structure at $k(\omega)$ close to $\pm\pi/s$ leads to very low bistability thresholds as compared to other structures. This is illustrated in example B of Fig. 5: Relative to the waveguide design in example A, the design in example B moves the resonance frequency deeper into the passing band thus decreasing the quality factor (18).

Summarizing, the inter-site structure of the resonant waveguide-resonator interaction schematically shown in Fig. 3 allows to achieve much higher values for the linear quality factor Q. As a consequence, much smaller bistability threshold intensities for the nonlinear transmission are obtained. To employ these advantages, the wavevector $k(\omega_{\rm res})$ of the guided mode at the resonance frequency $\omega_{\rm res}$, Eq. (16), should be as close as possible to π/s. This requirement coincides with the condition of a very small group velocity in the waveguide and provides us with a possibility to create low-threshold all-optical switching devices based on slow-light photonic crystal waveguides.

IV. CONCLUSIONS

We have presented a detailed analysis of the transmission properties of the PhC waveguides side-coupled to nonlinear resonators which may serve as a basic element of active photonic-crystal circuitry. We have suggested and developed a semi-analytical approach based on the effective discrete equations derived in the framework of a consistent Green's function formalism. This approach is ideally suited for a qualitative and semi-quantitative description of various types of photonic-crystal devices that involve a discrete set of small-volume cavities. We have shown that this novel approach allows to describe adequately the light transmission in the waveguide-resonator structures near the band edges. Specifically, we have demonstrated that the light transmission remains perfect at one of the band edges for the intersite coupled structure (see Fig. 3). These features allow a significant enhancement of the resonator quality factor and, accordingly, a substantial reduction of the bistability threshold. As a consequence, we refer to this type of nonlinearity enhancement as a *geometric enhancement*. The possibility of such enhancement is a direct consequence of the discreteness of the photonic crystal waveguide and is in a sharp contrast to similar resonant systems based on ridge waveguides. In addition, we would like to emphasize that the engineering of the geometry of photonic-crystal-based devices such as that presented

in Fig. 1 becomes extremely useful for developing novel concepts of all-optical switching in the *slow-light regime* of PhC waveguides which may have much wider applications in nanophotonics [20].

Acknowledgments

The work of Y.K. and A.E.M. has been supported by the Australian Research Council through the Center of Excellence Program. S.F.M. and K.B. acknowledge a support from the Center for Functional Nanostructures of the Deutsche Forschungsgemeinschaft within the project A1.1.

[1] H.M. Gibbs, *Optical bistability: Controlling light with light* (Academic Press, Orlando, 1985).

[2] K. Busch, S. Lölkes, R.B. Wehrspohn, and H. Föll (Eds.), *Photonic Crystals: Advances in Design, Fabrication, and Characterization* (Wiley-VCH, Berlin, 2004); K. Inoue and K. Ohtaka (Eds.), *Photonic Crystals: Physics, Fabrication and Applications* (Springer, Berlin, 2004).

[3] S. H. Fan, P. R. Villeneuve, and J. D. Joannopoulos, Phys. Rev. Lett. **80**, 960 (1998).

[4] Y. Xu, Y. Li, R. K. Lee, and A. Yariv, Phys. Rev. E **62**, 7389 (2000).

[5] M. Soljacic, M. Ibanescu, S. G. Johnson, Y. Fink, and J. D. Joannopoulos, Phys. Rev. E **66**, 055601(R) (2002).

[6] S. H. Fan, Appl. Phys. Lett. **80**, 908 (2002).

[7] M. F. Yanik, S. H. Fan, and M. Soljacic, Appl. Phys. Lett. **83**, 2739 (2003).

[8] P. Chak, S. Pereira, and J. E. Sipe, Phys. Rev. B **73**, 035105 (2006).

[9] A. R. Cowan and J. F. Young, Phys. Rev. E **68**, 046606 (2003).

[10] A. R. Cowan and J. F. Young, Semicond. Sci. Technol. **20**, R41 (2005).

[11] S. F. Mingaleev, Yu. S. Kivshar, and R. A. Sammut, Phys. Rev. E **62**, 5777 (2000).

[12] S. F. Mingaleev and Yu. S. Kivshar, Phys. Rev. Lett. **86**, 5474 (2001).

[13] S. F. Mingaleev and Yu. S. Kivshar, Opt. Lett. **27**, 231 (2002).

[14] S.F. Mingaleev and Yu.S. Kivshar, J. Opt. Soc. Am. B **19**, 2241 (2002).

[15] A. E. Miroshnichenko, S. F. Mingaleev, S. Flach, and Yu. S. Kivshar, Phys. Rev. E **71**, 036626 (2005).

[16] A. E. Miroshnichenko and Yu. S. Kivshar, Phys. Rev. E **72**, 056611 (2005).

[17] A. E. Miroshnichenko and Yu. S. Kivshar, Opt. Express **13**, 3969 (2005).

[18] S. F. Mingaleev, A. E. Miroshnichenko, Yu. S. Kivshar, and K. Busch Phys. Rev. E **74**, 046603 (2006).

[19] U. Fano, Phys. Rev. **124**, 1866 (1961).

[20] Yu. A. Vlasov and M. O'Boyle and H. F. Hamann and S. J. McNab, Nature **438**, 65 (2005).